Polymer Communication

Origin of the divergence of the timescales for volume and enthalpy recovery

Prashanth Badrinarayanan, Sindee L. Simon*

Department of Chemical Engineering, Texas Tech University, Box 43121, Lubbock, TX 79409-3121, USA

Abstract

Although the relationship between the relaxation timescales of thermodynamic, mechanical, viscoelastic, and dielectric properties in amorphous materials has been studied extensively, no general consensus has been reached. In this work, we examine the relationship between the timescales of volume and enthalpy relaxation for polystyrene using the cooling rate dependence of the glass transition temperature (T_g) obtained from capillary dilatometry and differential scanning calorimetry (DSC). Our analysis suggests that both volume and enthalpy exhibit similar relaxation timescales at temperatures above and below T_g. The divergence of the times required to reach equilibrium noted in the literature at temperatures several degrees below the nominal T_g is attributed to the effects of nonlinearity. The relationship between nonlinearity and dynamic heterogeneity is discussed.
© 2007 Published by Elsevier Ltd.

Keywords: Glass transition; Structural recovery; Relaxation timescales

1. Introduction

At temperatures lower than their glass transition temperatures (T_gs), glass forming materials deviate from equilibrium behavior and form glasses. As a consequence of the kinetic nature of the glass transition process, the deviation from equilibrium behavior depends on the cooling rate [1,2]. The kinetic nature of the glass transition is also exemplified by structural relaxation below the T_g, which refers to the process by which the thermodynamic properties of a material such as volume or enthalpy evolve with time in an effort to reach equilibrium [1–3]. Although structural relaxation has been studied extensively, seemingly discrepant results are found regarding the relationship between the relaxation timescales of different properties. Some reports suggest that different properties exhibit identical relaxation timescales or relaxation kinetics [4–18]; whereas, other studies imply that the timescales are dissimilar [19–30].

In an effort to better understand the relative timescales of different properties, Simon and coworkers [19] developed

a general picture for relaxation timescales. The general picture [19] shown in Fig. 1, depicts the temperature dependence of the times required to reach equilibrium (t_∞s) for selenium, polystyrene, and polyetherimide. The solid symbols represent the experimental data, whereas the open symbols represent extrapolated values of the times required to reach equilibrium determined from the Tool–Narayanaswamy–Moynihan (TNM) model [31–33] for polystyrene and from a linear extrapolation for selenium. Enthalpy, volume, and creep relaxation measurements for polyetherimide, shown as the grey symbols, suggest that the timescales for different properties are the same near and above the nominal value of T_g (defined as the temperature where the time to reach equilibrium is 10^4 s) [4]. The same trend can be observed from volume and enthalpy relaxation measurements for polystyrene [20]. However, at temperatures below T_g, TNM model [31–33] calculations suggest that the times required to reach equilibrium for volume and enthalpy diverge for polystyrene, with volume requiring a longer time compared to enthalpy [20]. A similar divergence was observed by Thurau and Ediger [21] for the times required to reach equilibrium during structural relaxation for the translational and rotational diffusion of a probe molecule in polystyrene, as shown in Fig. 1. The divergence

* Corresponding author. Tel.: +1 806 742 3553.
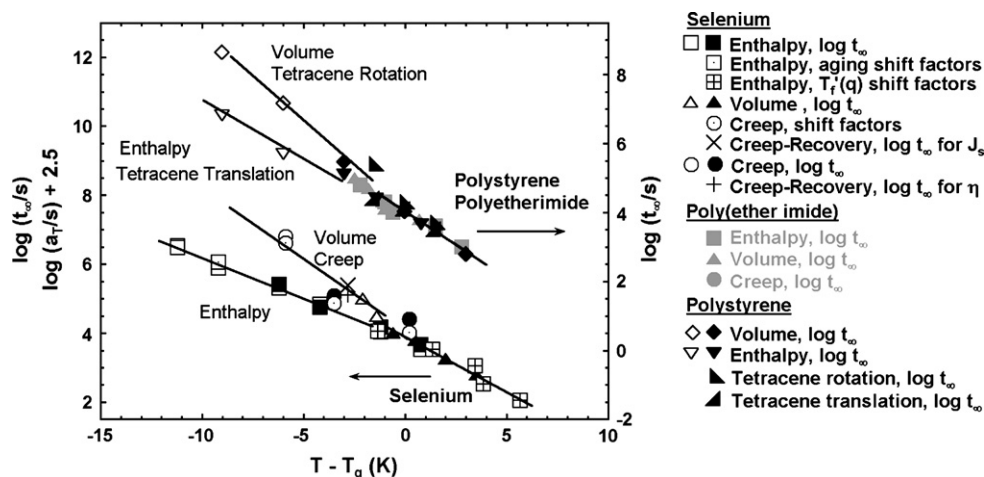 *E-mail address:* sindee.simon@ttu.edu (S.L. Simon).

Fig. 1. Temperature dependence of times required to reach equilibrium for selenium, polyetherimide, and polystyrene, after Ref. [19]. Note that in that work, the volume relaxation data for selenium were obtained from Ref. [34]. Experimental data of Thurau and Ediger from Ref. [21] for the times required to reach equilibrium for tetracene rotation and translational diffusion in polystyrene are also shown.

in timescales is also observed in selenium: the times to reach equilibrium for volume relaxation obtained from the data of Hamada and coworkers [34] are found to be similar to the timescales of creep and enthalpy relaxation at temperatures above T_g; however, below T_g, volume and creep require a longer time to reach equilibrium compared to enthalpy [19]. Hence, according to the general picture [19], different properties have the same relaxation time close to the nominal value of T_g; however, several degrees below the nominal T_g, volume requires a longer time to attain equilibrium compared to enthalpy, resulting in a divergence in the relaxation timescales.

Although the general picture presented in Fig. 1 is consistent with the majority of previous works, a closer review of the literature reveals that perhaps the divergence in the times required to reach equilibrium for volume, enthalpy, and creep below T_g is due to the nonlinearity of the temperature jumps made to obtain data at these temperatures rather than simply due to low aging temperatures themselves, as indicated by Fig. 1. For example, a divergence in timescales for different properties has been observed in studies in which the times required to reach equilibrium were examined or modeled after down-jumps of greater than several degrees [19−27] − the only exceptions to this are four papers [4−7]. The first two of these [4,5] are work from Simon, Plazek, and coworkers on polyetherimide in which the same relaxation times were found for enthalpy, volume, and creep in spite of fairly large temperature down-jumps; however, in those works, the aging temperatures were still in the vicinity of the nominal T_g as shown in Fig. 1, explaining why the timescales were similar, i.e., the jumps were not large enough that the nonlinearity became an issue. In the third paper by Rault [6] on polystyrene and poly(vinyl acetate), volume and enthalpy recovery were compared; at least in the polystyrene case, comparisons were made at temperatures where again the jump size is such that the two properties are expected to be the same based on our previous results, shown in Fig. 1. In the fourth paper, Bero and Plazek [7] made small 2.5 K jumps to temperatures

approximately 10 K below the nominal T_g in a specific attempt to reduce the nonlinearity of the jumps; as an aside, it is noted that, depending on the material, 2.5 K jumps are not necessarily small enough to achieve nearly linear behavior: Moynihan and coworkers [22] observed that the times required to reach equilibrium for enthalpy and the index of refraction differed after 2.8 K jumps in B_2O_3. In contrast to the results involving down-jumps to compare the times required to reach equilibrium, studies in which similar responses for various properties were observed often involved comparing the relaxation times of different properties at equilibrium density (above T_g) or comparing the cooling rate dependence of T_g or T_f' for different properties; in all such studies [8−13,28], relaxation times were similar and showed the same Vogel [35]−Tamman−Hesse [36]−Fulcher [37] temperature dependence although there were some slight discrepancies: Sasabe and Moynihan [28] pointed out that for poly(vinyl acetate), the glass transition temperature for volume was 1 K lower than that for enthalpy measured at the same rate; similarly, Moon and coworkers [8] found that although the relaxation times for enthalpy and dielectric spectroscopy agreed quantitatively for a low molecular weight poly(propylene glycol), there was a systematic difference in the enthalpic and dielectric α-relaxation times for a higher molecular weight sample; Roland and coworkers [9] also found that highly crosslinked polyvinyl-ethylenes showed different enthalpic and dielectric relaxation times. The remaining papers, which do not fit into either of the above categories, are those in which the kinetics of, for example, volume and enthalpy recovery are compared; most of these works argue that enthalpy and volume are directly related because the ratio of their relative relaxation rates (dh/dv) is a constant at a given aging temperature after down- or up temperature jumps [14−18]; however, others find that the kinetics of structural recovery for the two properties are considerably different after more complicated temperature or pressure histories [29,30]. We have previously argued that one cannot determine whether the timescales for various

properties are related based on their kinetics [4]; rather the times required to reach equilibrium or the relaxation times at equilibrium should be compared.

The origin of the divergence of the timescales required for different macroscopic properties to reach equilibrium has been suggested by Thurau and Ediger [21,38] to be related to dynamic spatial heterogeneities [38–44] based on the supposition that the divergence of rotational and translational diffusion timescales is due to the presence of dynamic spatial heterogeneities. Modeling work by Diezemann [45] supports this hypothesis. In addition, an enthalpy landscape analysis by Lacks and coworkers [46] also predicts a difference between, for example, the times required to reach equilibrium for enthalpy and volume. Our hypothesis that it is the nonlinearity of down or up temperature jumps that leads to this divergence will be tested in this work for polystyrene using measurements of the cooling rate dependence of T_g from capillary dilatometry and differential scanning calorimetry (DSC). We will show that indeed, the T_g values from volume and enthalpic measurements, and their cooling rate dependence, are similar. The implications of the results, including whether they imply a relationship between nonlinearity and dynamic heterogeneity will then be discussed.

2. Experimental

2.1. Material

The experiments in this work were performed using polystyrene (Dylene 8) obtained from Arco Polymers. The same material was used in previous volume and enthalpy relaxation studies by Simon and coworkers [20,47–49].

2.2. Dilatometric studies

The dilatometric studies were conducted using a capillary dilatometer constructed following the design of Bero and Plazek [7] and Bekkedahl [50] in which mercury is used as the confining fluid. The design of the capillary dilatometer is explained in detail elsewhere [47,48,51]. The 5.0 g polystyrene sample was molded under vacuum into a cylinder of 1.27 cm diameter; a 0.3 cm axial hole was drilled through the entire length of the sample to facilitate better contact with the confining fluid. The experiments were performed by placing the dilatometer in a temperature controlled oil bath (Model 6025, Hart scientific) filled with silicone oil. A platinum resistance thermometer (Black Stack 1560, Hart Scientific) with an accuracy of 0.0013 K was used to measure the bath temperatures. A linear variable differential transformer (LVDT) was used to track the change in mercury level with temperature [52]. An overall resolution of 0.4×10^{-5} cm^3/g was obtained by minimizing noise through a low pass filter [47].

The dilatometric cooling experiments were performed from an initial temperature of 105 °C to a final temperature of 60 °C using cooling rates from 0.2 to 0.01 K/min. The cooling run at 0.003 K/min was performed from an initial temperature of 97.5 °C to reduce run time; note that the sample was at equilibrium density before commencing the cooling run at 0.003 K/min. The thermal lags for the cooling experiments were calculated based on the method of Simon [53] and found to be 0.1 K for a cooling rate of 0.2 K/min and much lower at slower cooling rates; hence, no corrections were made to the experimental data. T_g was determined from the volume versus temperature curves by the point of intersection of the extrapolated glass line with the equilibrium liquid line. The standard deviation of dilatometric T_g values is ± 0.2 °C based on repeated measurements performed at cooling rates of 0.1 and 0.03 K/min.

2.3. DSC studies

The DSC studies were conducted using a Perkin–Elmer Pyris 1 DSC equipped with an ethylene glycol cooling system maintained at 5 °C. A thin sample with a thickness of 0.27 mm was used in the experiments. All experiments were performed under a nitrogen atmosphere. The temperature calibrations on cooling were performed using two liquid crystal standards, (+)-4-*n*-hexylophenyl-4′-(2′-methylbutyl)-biphenyl-4-carboxylate (CE-3 from Menczel and Leslie [55], University of Alabama; smectic to cholesteric transition at 78.8 °C) and 4,4-azoxyanisole (Sigma–Aldrich Co. Ltd.; liquid crystal to isotropic liquid transition at 134.5 °C). Heat flow calibrations on cooling were performed using indium [56]. The calorimetric cooling runs were performed using cooling rates from 30 to 2 K/min. The fast cooling runs at 30 and 20 K/min were performed from 170 to 60 °C in order to ensure that the instrumental cooling rate was well controlled at T_g, whereas the other runs were performed from 130 to 60 °C. Due to the thin geometry of the DSC sample the thermal lag was found to be only 0.04 °C at 30 K/min and lower at slower cooling rates; hence, no corrections were made to the experimental data. The glass transition temperatures were obtained from the heat flow versus temperature curves using the half height criteria in Pyris software. The standard deviation of calorimetric T_g values is ± 0.3 °C based on two or three measurements performed at each cooling rate.

2.4. Model calculations

The TNM model [31–33] parameters x, β, $\ln(A)$, and $\Delta h/R$ were estimated for dilatometry from a simultaneous fit of the data obtained using cooling rates from 0.2 to 0.003 K/min. The fictive temperatures (T_fs) resulting from the model calculations were used to calculate the specific volume:

$$v = v_\infty + v_\infty \Delta\alpha (T_f - T) \tag{1}$$

where $\Delta\alpha$ refers to the difference in thermal expansivity between the liquid and the glassy states and v_∞ is the equilibrium specific volume. The Levenberg–Marquardt algorithm in Matlab® software was used to optimize the parameters x, β, and $\ln(A)$ for various fixed values of $\Delta h/R$; the final value of $\Delta h/R$ was taken as that corresponding to the minimum value

of chi square of the fit [57]. The step size in the program was varied to ensure that the maximum change in T_f was not more than 0.1 K.

For DSC, the temperature dependence of the fictive temperature (T_f) obtained from model calculations was used to calculate the absolute heat capacity:

$$C_p(T) = C_{pg}(T) + \Delta C_p(T_f)\frac{dT_f}{dT} \tag{2}$$

where $\Delta C_p(T_f)$ refers to the difference in liquid and glassy heat capacities, C_{pl} and C_{pg} at T_f. In order to fit the DSC data with the TNM model [31–33], the normalized heat capacity (C_{PN}) data obtained from DSC cooling runs were transformed to absolute heat capacity as shown below:

$$C_p(T) = C_{PN}(C_{pl}(T) - C_{pg}(T)) + C_{pg}(T) \tag{3}$$

The equations for the liquid and glassy heat capacities were determined from a step scan procedure [58] and depend on the temperature as follows:

$$C_{pl}(T) = 0.70 + 0.0031T(\mathrm{K}) \quad \mathrm{J\,g^{-1}\,K^{-1}} \tag{4}$$

$$C_{pg}(T) = 0.02 + 0.0041T(\mathrm{K}) \quad \mathrm{J\,g^{-1}\,K^{-1}} \tag{5}$$

In order to estimate the optimum model parameters, the data obtained on cooling at 30, 10, 4, and 2 K/min were fit simultaneously using a computer program while ensuring that the change in T_f was less than 0.1 K between steps.

For the fits to both the dilatometric and calorimetric data, the error in each model parameter was determined by varying that parameter and determining chi square while maintaining the other parameters constant. The errors were evaluated as the change in a parameter which results in a chi square 1% greater than the minimum value. Errors were also calculated from the covariance matrix of the optimized fit parameters, since the diagonal elements of the covariance matrix represent the square of the standard error of the fit parameters [59,60]. The errors determined from this method were at least two times smaller compared to the errors determined from chi square method; the errors reported are those from the chi square method.

3. Results

The dilatometric curves obtained on cooling at various rates are shown in Fig. 2a. The fits of the TNM model [31–33] to these volumetric data are shown as the dotted lines in Fig. 2a. The heat capacity response obtained on cooling at various rates from 30 to 2 K/min is shown in Fig. 2b, with the dotted line representing the fits of the TNM model [31–33]. The model provides an excellent description of the data for both capillary dilatometry and DSC. The parameters obtained from the best fit of the dilatometric and calorimetric data are tabulated in Table 1, along with values obtained by fitting both cooling and heating data in other work [54]. For
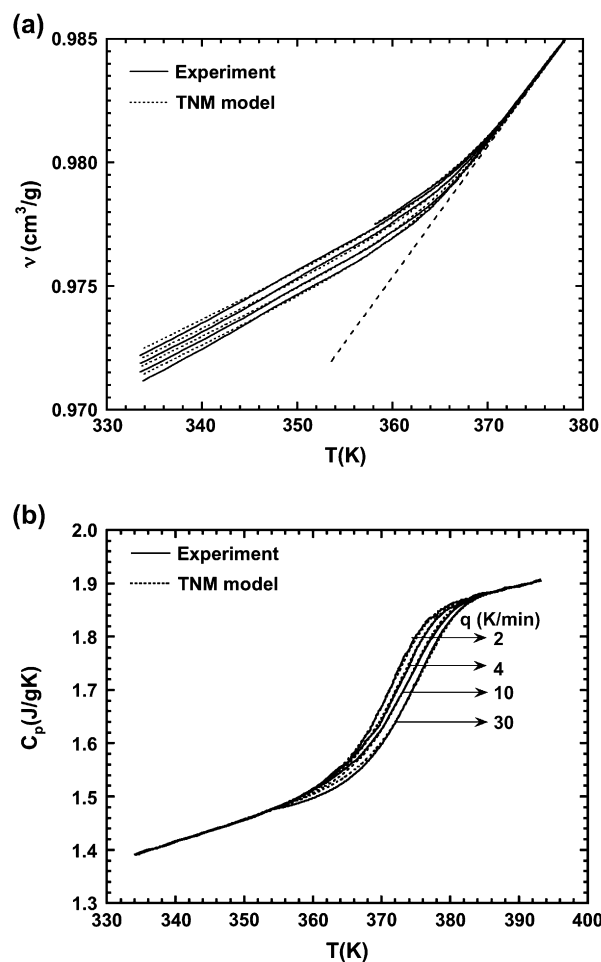
Fig. 2. (a) Specific volume versus temperature response obtained on cooling at various rates (q) from capillary dilatometry. The dashed line represents the equilibrium liquid line. The dotted lines represent the fit of the TNM model. (b) Heat capacity response as a function of cooling rate (q) from transformed DSC data (solid lines) and TNM model calculations (dotted lines).

both dilatometry and calorimetry, the model parameters are found to vary with thermal history, as is widely reported in the literature [61]. The significance of the model parameters will be discussed in more detail later.

The cooling rate dependence of T_g from dilatometry and DSC is plotted in Fig. 3 along with the temperature dependence of the times required to reach equilibrium (t_∞) for volume and enthalpy relaxation from previous work. The solid circles and solid inverted triangles represent volume and enthalpy relaxation measurements from Simon et al. [20]. The solid right triangles represent more recent enthalpy relaxation measurements from our laboratory [49] and include error bars from that work; the error in t_∞ is almost negligible below aging temperatures of 100 °C but is considerable at higher temperatures due to the small changes in enthalpy and short timescales involved. The T_g values from dilatometry and calorimetry are represented by squares and triangles, respectively, in Fig. 3. The solid lines represent the best fits to the T_g data from dilatometry and DSC. The dashed line in Fig. 3 represents the time required to reach equilibrium calculated from

Table 1
Comparison of TNM model parameters for capillary dilatometry and DSC data

Parameter	This work		Simultaneous fits of cooling and heating [54]	
	Dilatometry	DSC	Dilatometry	DSC
$\Delta h/R$ (kK)	151.2 ± 1.3	96 ± 0.7	130.1 ± 0.8	82.7 ± 0.9
$\ln(A/s)$	-402.7 ± 0.03	-253.8 ± 0.02	-344.7 ± 0.02	-217.1 ± 0.02
x	0.723 ± 0.01	0.790 ± 0.01	0.258 ± 0.002	0.426 ± 0.006
β	0.199 ± 0.004	0.424 ± 0.005	0.451 ± 0.002	0.602 ± 0.005

the following Vogel [35]–Tamman–Hesse [36]–Fulcher [37] equation:

$$\log\left(\frac{t_\infty}{t_{\infty,\mathrm{ref}}}\right) = \log A + \frac{C}{2.303(T - T_\infty)} \tag{6}$$

where the values of the constants are taken from previous work [20]: $\log A = -12.8$, $t_{\infty,\mathrm{ref}} = 2512$ s, $T_\infty = 69.8\ ^\circ$C, and $C = 852.11$ K. The temperature dependence of the times to reach equilibrium calculated from the VTHF equation is in agreement with the experimental values above the nominal glass transition temperature for this material ($T_g \approx 95\ ^\circ$C). On the other hand, below T_g, the values of t_∞ calculated from VTHF equation are higher than the experimental values, consistent with previous experimental work at equilibrium density [19,20,49,62–67] and theoretical [68–70] work, although we note that in some reports [10,64,71,72], no deviation from VTHF behavior is observed at temperatures below T_g; a more detailed discussion can be found elsewhere [64].

The value of the slope, $dT_g/d(-\log q)$, in Fig. 3 is found to be 2.5 ± 0.1 K when the volume and enthalpy data are evenly weighted and taking into account that the T_g value for dilatometry is 1.0 K lower than that for calorimetry at the same rate, similar to the observation of Sasabe and Moynihan [28] for poly(vinyl acetate).[1] The value of $dT/d(\log t_\infty)$ obtained from a linear fit of all the relaxation data is found to be 2.7 ± 0.2 K, and the value obtained from the VTHF Eq. (6) [35–37] is 2.5 K at 100 $^\circ$C. Agreement between the temperature dependence of times required to reach equilibrium, $dT/d(\log t_\infty)$, for enthalpy relaxation and the cooling rate dependence of T_f' from enthalpy measurements were similarly observed for selenium [19]. However, as mentioned earlier, in that same work, the timescales for creep and volume measurements were found to diverge from those for enthalpy at temperatures a few degrees below the nominal value of T_g [19], and a similar result was suggested for polystyrene based on the temperature dependence of volume and enthalpy shift factors and also from TNM model [31–33] calculations [20]. In this work, no obvious divergence can be observed between the timescales of volume and enthalpy.

---

[1] The fact that the dilatometric T_g is 1 K lower than the enthalpic T_g is based on (i) the best fit of the T_g versus log q data and (ii) the fact that T_f' values obtained on heating after cooling at a given rate are also lower for volume than for enthalpy [54].
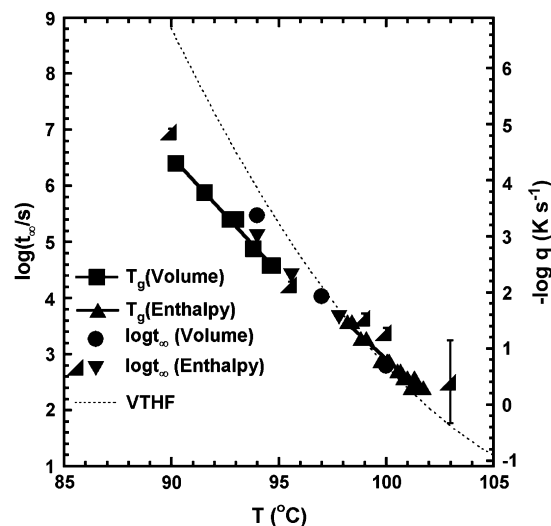

Fig. 3. Comparison of the temperature dependence of the times required to reach equilibrium (t_∞) for enthalpy and volume relaxation of Dylene 8 with the cooling rate dependence of T_g for these same properties. The times required to reach equilibrium (t_∞) are taken from Ref. [20] (● ▼) and Ref. [49] (◢). Error bars from Ref. [49] are also included but are only easily visible for the highest aging temperature. The dashed line represents the time to reach equilibrium calculated from the VTHF equation.

The cooling rate dependence of T_g and the temperature dependence of the relaxation time can be used to calculate the apparent normalized apparent activation energy ($\Delta h/R$):

$$\frac{\Delta h}{R} = \frac{d\ln\tau}{d(1/T)} \approx -\frac{d\ln q}{d(1/T_g)} \tag{7}$$

where q is the cooling rate and τ is the relaxation time at temperature T. The value of $\Delta h/R$ evaluated from only the T_g measurements in dilatometry (127 ± 5 kK) is similar to the corresponding value of $\Delta h/R$ obtained only from the DSC data (112 ± 6 kK). The relationship between the values of $\Delta h/R$ from dilatometry and DSC is further ascertained from a t-test performed at 90% confidence interval. Based on the t-test, the value of $\Delta h/R$ from T_g measurements in dilatometry is found to statistically similar to the value of $\Delta h/R$ from DSC studies, which substantiates the lack of any divergence in the timescales. However, the value of $\Delta h/R$ from TNM model fits of the cooling data is found to be 58% greater for dilatometry, since the parameters are strongly dependent on the thermal history of the data being fit, as shown in Table 1.

4. Discussion

In this work, the volume and enthalpy data overlap over the entire temperature range. Although the T_g values from dilatometry are slightly lower (1 K) than the values from DSC for the same cooling rate, it is clear that there is no divergence in T_g measurements based on volume and enthalpy, in contradiction to the original prediction from TNM model calculations [20] and the general picture shown in Fig. 1 [19]. The primary difference between these works is that the

measurements in this work were performed on cooling, and hence, the degree of nonlinearity in the measurements is considerably smaller than for large temperature down-jumps. Consequently, we suggest that the divergence observed in our earlier work at aging temperatures several degrees below the nominal T_g value arises from the nonlinearity of structural relaxation coupled with the fact that volume relaxation is considerably more nonlinear than enthalpy relaxation [20]. Hence, for large temperature jumps, volume relaxation is expected to exhibit longer relaxation timescales, which would lead to the observed divergence in the timescales.

Although it has long been known that the magnitude of the temperature jump affects the time required to reach equilibrium for up-jumps [73], conventional wisdom, based on Kovacs' seminal work [73], has dictated that the magnitude of the temperature jump does not affect the time required to reach equilibrium for down-jumps. Although Kovacs' volume recovery plots indicate that the curves for down-jumps merge as equilibrium is reached, the times required to reach equilibrium for the shortest jumps cannot be discerned as the data at long times for these jumps are not explicitly shown. Furthermore, recent results from our laboratory [47,51] clearly depict the dependence of the time required to reach equilibrium on the magnitude of down-jumps for volume relaxation, with t_∞ increasing for larger jumps. Hence, the divergence of the timescales required to reach equilibrium for volume and enthalpy at low aging temperatures is suggested to be due to differences in the degree of nonlinearity for the relaxation of these two properties.

Furthermore, differences in the nonlinearity of volume and enthalpy recovery are clearly evidenced by differences in the nonlinearity parameter x in the TNM [31–33] and Kovacs–Aklonis–Hutchinson–Ramos (KAHR) [74] models. Although these phenomenological models of structural recovery are known to have shortcomings [48,53,61,75,76] and erroneously predict that the time required to reach equilibrium is independent of the magnitude of down-jumps, they do describe the nonlinearity of structural relaxation. For example, in the TNM model [31–33], the nonlinearity parameter x is incorporated in the expression for relaxation time (τ) as shown below:

$$\ln(\tau) = \ln(A) + \frac{x\Delta h}{RT} + \frac{(1-x)\Delta h}{RT_f} \qquad (8)$$

where $\Delta h/R$ is the relative apparent activation energy, T_f is the fictive temperature corresponding to the temperature T, A is a constant, and the nonlinearity parameter x accounts for the

structure dependence of the relaxation time in the glassy state. The values of x obtained by fitting the dilatometric and calorimetric data in this work are compared with the values reported in the literature [14,20,47,49,54,57,77–79] in Table 2. The pronounced nonlinearity of volume relaxation is clearly evident from the fact that the values of the nonlinearity parameter x obtained from dilatometry are lower than the values from calorimetry. Although the values of the x obtained from fitting dilatometric and calorimetric cooling data in this work differ from the values obtained from simultaneous fits of cooling and heating data in other work [54] and from those obtained on fitting volume and enthalpy relaxation data [20,47,49], it is clear that the range of the nonlinearity parameter is lower for dilatometry than for calorimetry indicating that volume relaxation will be more nonlinear than enthalpy relaxation for a given temperature jump.

In sum, we suggest that the divergence in timescales observed for macroscopic properties after nonlinear temperature jump experiments below T_g is due to differences in the degree of nonlinearity for the structural relaxation of different properties. Consequently, experiments in which this nonlinearity is minimized, including cooling experiments which provide T_g as a function of cooling rate as we have performed in this work, show that the timescales are similar for volume and enthalpy. On a molecular level, since the divergence of the timescales has been related experimentally to dynamic heterogeneities [21,38] and by modeling to the energy [45] or enthalpic landscapes [46], it is pertinent to ask whether dynamic heterogeneity and the energy/enthalpy landscape ideas are able to account for and model the differences in nonlinearity observed, for example, for enthalpy and volume recovery. We note that in the enthalpic landscape analysis of Lacks and coworkers [46], the asymmetry of approach experiment is attributed to history-dependent weighting factors rather than to the dependence of the relaxation time(s) on instantaneous structure; hence, the nonlinearity of the relaxation response may arise from dynamic heterogeneity rather than being due to the changing structure (volume, enthalpy) of the glass. In fact, agreement between the timescales of volume and enthalpy for small linear temperature jumps is predicted by the enthalpy landscape model since for linear jumps, enthalpy would be a linear function of volume [80].

5. Conclusions

The glass transition temperature of polystyrene was determined as a function of cooling rate using both capillary dilatometry and DSC. The data were used to reanalyze the origin of the divergence in the timescales required to reach equilibrium for volume and enthalpy relaxation at temperatures below the nominal T_g, which has been the subject of considerable debate. In this work, the relationship between T_g and the logarithm of the cooling rate was found to be the same for the two properties even for temperatures 10 K below the nominal glass transition temperature, and no divergence could be observed between volume and enthalpy. The lack of divergence in this work is attributed to the reduced degree of

Table 2
Comparison of the values of the nonlinearity parameter for polystyrene

Source	Dilatometry	DSC
This work	0.723	0.792
Simon et al. [20]	0.1	0.36
Bernazzani and Simon [47]	0.2	
Badrinarayanan et al. [54]	0.258	0.426
Hadac et al. [14]	0.36–0.56	0.56–0.72
Refs. [49,57,77–79]		0.37–0.48

nonlinearity of the measurements on cooling. The divergence observed in earlier work for the times required to reach equilibrium at aging temperatures below T_g is attributed to the pronounced nonlinearity of volume relaxation compared to enthalpy relaxation coupled with relatively large temperature down-jumps used for the lower aging temperatures. A relationship between nonlinearity and dynamic heterogeneity is suggested.

Acknowledgement

References

[1] Plazek DJ, Ngai KL. In: Mark JE, editor. Physical properties of polymers handbook. NY: American Institute of Physics; 1996 [chapter 12].

[2] McKenna GB. In: Booth C, Price C, editors. Comprehensive polymer science, polymer properties, vol. 2. Oxford: Pergamon Press; 1989 [chapter 10].

[3] McKenna GB, Simon SL. In: Cheng SZD, editor. Handbook of thermal analysis and calorimetry, applications to polymers and plastics, vol. 3. Elsevier Science; 2002 [chapter 2].

[4] Simon SL, Plazek DJ, Sobieski JW, McGregor ET. J Polym Sci Part B Polym Phys 1997;35:929.

[5] Echeverria I, Su P-C, Simon SL, Plazek DJ. J Polym Sci Part B Polym Phys 1995;33:2457.

[6] Rault J. J Phys Condens Matter 2003;15:S1193.

[7] Bero CA, Plazek DJ. J Polym Sci Part B Polym Phys 1991;29:39.

[8] Moon IK, Jeong YH, Furukawa T. Thermochim Acta 2001;377:97.

[9] Robertson CG, Santangelo PG, Roland CM. J Non-Cryst Solids 2000;275:153.

[10] Andreozzi L, Faetti M, Zulli F, Giordano M. Macromolecules 2004;37: 8010.

[11] Jeong YH, Moon IK. Phys Rev B 1995;52:6381.

[12] Carpentier L, Descamps M. J Phys Chem B 2003;107:271.

[13] Moynihan CT, Easteal AJ, DeBolt MA, Tucker J. J Am Ceram Soc 1976;59:12.

[14] Hadac J, Slobodian P, Riha P, Saha P, Kubat J, Rychwalski RW, et al. J Non-Cryst Solids, in preparation.

[15] Mijovic J, Ho T. Polymer 1993;18:3865.

[16] Oleinik EF. Polym J 1987;19:105.

[17] Slobodian P, Riha P, Rychwalski RW, Emri I, Saha P, Kubat J. Eur Polym J 2006;42:2824.

[18] Malek J, Montserrat S. Thermochim Acta 1998;313:191.

[19] Echeverria I, Kolek PL, Plazek DJ, Simon SL. J Non-Cryst Solids 2003;324:242.

[20] Simon SL, Sobieski JW, Plazek DJ. Polymer 2001;42:2555.

[21] Thurau CT, Ediger MD. J Chem Phys 2002;116:9089.

[22] DeBolt MA, Easteal AJ, Macedo PB, Moynihan CT. J Am Ceram Soc 1976;59:16.

[23] Cowie JMG, Harris S, McEwen LJ. Macromolecules 1998;31:2611.

[24] Cowie JMG, Ferguson R, Harris S, McEwen LJ. Polymer 1998;39:4393.

[25] McKenna GB, Letterier Y, Schultheisz CR. Polym Eng Sci 1995;35:403.

[26] Roe RJ, Millman GM. Polym Eng Sci 1983;23:318.

[27] Perez J, Cavaille JY, Calleja RD, Ribelles JLG, Pradas MM, Greus AR. Macromol Chem 1991;192:2141.

[28] Sasabe H, Moynihan CT. J Polym Sci Part B Polym Phys 1978;16:1447.

[29] Adachi K, Kotaka T. Polym J 1982;14:959.

[30] Weitz A, Wunderlich B. J Polym Sci Part B Polym Phys 1974;12:2473.

[31] Tool AQ. J Am Ceram Soc 1946;29:240.

[32] Narayanaswamy OS. J Am Ceram Soc 1971;54:491.

[33] Moynihan CT, Macedo PB, Montrose CJ, Gupta PK, DeBolt MA, Dill JF, et al. Ann NY Acad Sci 1976;279:15.

[34] Hamada S, Sato T, Shirai T. Bull Chem Soc Jpn 1968;41:135.

[35] Vogel H. Phys Z 1921;22:645.

[36] Tamman G, Hesse G. Z Anorg Allg Chem 1926;156:245.

[37] Fulcher GS. J Am Chem Soc 1925;8:339 and 789.

[38] Thurau CT, Ediger MD. J Polym Sci Part B Polym Phys 2002;40: 2463.

[39] Richert R. J Phys Condens Matter 2002;14:R703.

[40] Ediger MD. Ann Rev Phys Chem 2000;51:91.

[41] Glotzer SC. J Non-Cryst Solids 2000;274:342.

[42] Bohmer R. Phase Transitions 1998;65:211.

[43] Bohmer R. Curr Opin Solid State Mater Sci 1998;3:378.

[44] Silescu H, Bohmer R, Diezemann G, Hinze G. J Non-Cryst Solids 2002;307:16.

[45] Diezemann G. J Chem Phys 2005;123:204510.

[46] Lei Y, Cummins K, Lacks DJ. J Polym Sci Part B Polym Phys 2003;41: 2302.

[47] Bernazzani P, Simon SL. J Non-Cryst Solids 2002;307:470.

[48] Simon SL, Bernazzani P. J Non-Cryst Solids 2006;352:4763.

[49] Li Q, Simon SL. Polymer 2006;47:4781.

[50] Bekkedahl N. J Res Natl Bur Stand 1949;42:145.

[51] Kolla S, Simon SL. Polymer 2005;46:733.

[52] Duran R, McKenna GB. J Rheol 1990;34:813.

[53] Simon SL. Macromolecules 1997;30:4056.

[54] Badrinarayanan P, Zheng W, Li Q, Simon SL. J Non-Cryst Solids, submitted for publication.

[55] Menczel JD, Leslie TM. Thermochim Acta 1990;166:309.

[56] Sarge SM, Hohne GWH, Cammenga HK, Eysel W, Gmelin E. Thermochim Acta 2000;361:1.

[57] Hodge IM, Huvard GS. Macromolecules 1983;16:371.

[58] Huang D, Simon SL, McKenna GB. J Chem Phys 2005;122:084907.

[59] Press WH, Flannery BP, Teukolsky SA, Vetterling WT. Numerical recipes in C++: the art of scientific computing. Cambridge: Cambridge University Press; 2002.

[60] Bard Y. Nonlinear parameter estimation. Academic Press; 1974.

[61] Hodge IM. J Non-Cryst Solids 1994;169:211.

[62] O'Connell PA, McKenna GB. J Chem Phys 1999;110:11054.

[63] Thurau CT, Ediger MD. J Chem Phys 2003;118:1996.

[64] Shi X, Mandanici A, McKenna GB. J Chem Phys 2005;123:174507.

[65] Algeria A, Echevarria EG, Telleria I, Colmenero J. Phys Rev B 1993;47: 14857.

[66] Cangialosi D, Wubbenhorst M, Schut H, van Veen A, Picken SJ. Phys Rev B 2004;69:134206.

[67] Lunkenheimer P, When R, Schenider U, Loidl A. Phys Rev Lett 2005;95: 055702.

[68] Dimarzio EA, Yang AJM. J Res Natl Inst Stand Technol 1997;102:135.

[69] Schweizer KS, Saltzman EJ. J Chem Phys 2003;119:1181.

[70] Dudowicz J, Freed KF, Douglas JF. J Chem Phys 2006;124:064901.

[71] Wagner H, Richert R. Polymer 1997;38:255.

[72] Alegria A, Echevarria EG, Goitiandia L, Telleria I, Colmenero J. Macromolecules 1995;28:1516.

[73] Kovacs AJ. Adv Polym Sci 1963;3:394.

[74] Kovacs AJ, Aklonis JJ, Hutchinson JM, Ramos AR. J Polym Sci Part B Polym Phys 1979;17:1097.

[75] Hodge IM. Macromolecules 1986;19:936.

[76] Hodge IM. Macromolecules 1987;20:2897.

[77] Weyer S, Merzylakov M, Schick C. Thermochim Acta 2001;377:85.

[78] Hutchinson JM, Ruddy M. J Polym Sci Part B Polym Phys 1988;26: 2341.

[79] Privalko VP, Demchenko SS, Lipatov YS. Macromolecules 1986;19:901.

[80] Lacks DJ. Case Western Reserve University, personal communication.